Microchemical Journal 170 (2021) 106665

Contents lists available at ScienceDirect

Microchemical Journal

journal homepage: www.elsevier.com/locate/microc

Synergistic effect of lacunary polyoxotungstates and carbon nanotubes for extraction of organophosphorus pesticides

Mahmood Akbari, Masoud Mirzaei *, Amirhassan Amiri *

Department of Chemistry, Faculty of Science, Ferdowsi University of Mashhad, PO Box 9177948974, Mashhad, Iran

ARTICLE INFO

Keywords:
Organophosphorus pesticides
Polyoxometalates
Lacunary polyoxotungstates
Carbon nanotube
Fruit juices
Water samples

ABSTRACT

In this work, for the first time, a nanocomposite composed of carbon nanotubes and lacunary polyoxotungstates (LPOT/CNT) was synthesized. The nanocomposites were used as a sorbent for the dispersive micro solid-phase extraction (D-μSPE) of five organophosphorus pesticides (OPPs) (*i.e.* fenthion, diazinon, fenitrothion, profenofos, and phosalone) from water and fruit juice samples. The extracted OPPs were quantified *via* gas chromatography-flame ionization detector (GC–FID). The main factors affecting the D-μSPE of the OPPs, such as the desorption conditions, amount of sorbent, and extraction time, were investigated, in detail. The LPOT/CNT nanocomposite shows a synergistic effect and its extraction efficiency is higher than intact CNTs and LPOTs. Under the optimized conditions, the D-μSPE-GC-FID method showed linearity from 0.02 to 200 ng mL^{-1}, limits of detection in the range of 0.007–0.02 ng mL^{-1}. The precision expressed as relative standard deviations (RSD%) ranged from 3.3 to 4.7%. The D-μSPE-GC-FID based on LPOT/CNT sorbent was used for the extraction of OPPs in fruit juices (apple juice and peach juice) and real water samples (wastewater and river water) and with relative recovery values of 94.2–99.6%.

1. Introduction

Organophosphorus pesticides (OPPs) are widely used in agricultural activities due to better control of pests and faster degradation in the environment. But, one of the sources of environmental pollution is trace OPP residues in aqueous samples and agricultural products as a result of excessive use which can be harmful to human health [1]. So, an efficient and reliable analytical method is required for the determination of OPPs in various real samples. However, due to the complexity of matrices and trace concentration of OPPs in real samples, extraction, and pre-concentration steps as necessary [2–4].

Until today, several extraction methods such as magnetic solid-phase extraction (MSPE) [7,8], solid-phase microextraction (SPME) [6], solid-phase extraction (SPE) [5], hollow-fiber liquid-phase microextraction (HF-LPME) [11], dispersive liquid-liquid microextraction (DLLME) [9,10], have been used to extract of OPPs. Dispersive micro solid-phase extraction (D-μSPE) is the simplest sample treatment approach, in which for the extraction of analytes, the sorbent is dispersed in the sample solution and collected centrifugally thereafter. Extraction efficiency increases due to the increase in the contact surface between the sorbent and the analytes [12–14]. The sorbent is a key part for the extraction ability of D-μSPE. Various sorbents such as metal-organic frameworks (MOFs) [15,16], conductive polymers (CPs) [17,18], molecularly imprinted polymers (MIP) [19], and carbon nanotubes (CNTs) [20] are used in the D-μSPE method. Due to the unique properties of polyoxometalates (POMs), these compounds have attracted wide attention as sorbents in recent years. The POMs are metal oxide clusters made from niobium, tantalum, vanadium, and tungsten at their highest oxidation states (+4, +5, +6) [21–26]. Due to their unique properties, POMs are widely used in the fields of medicine, magnetism, data storage, bioactivities, sensing, and catalysis, and sorbent. POMs as inorganic ligands that are more thermally and oxidatively stable than organic ligands [27–34]. Keggin type POMs has received much attention in recent years due to their unique chemical and physical properties [35]. Modification of the Keggin-type POMs that are prepared in appropriate chemical conditions such as temperature, pH, and concentration leads to the loss of one or more metal centers, which leads to the production of compounds called lacunary POMs (LPOMs) [36]. The lacunary polyoxotungstates (LPOTs) are a subset of LPOMs with a series of special properties such as thermal stability, multicentricity, oxidative, and rigidity [37–39]. Also, LPOMs with oxo-enriched surfaces, highly electronegative, and controllable size and shape are expected to be good

* Corresponding authors.
E-mail addresses: mirzaeesh@um.ac.ir (M. Mirzaei), ah.amiri@um.ac.ir (A. Amiri).

https://doi.org/10.1016/j.microc.2021.106665
Received 4 May 2021; Received in revised form 9 July 2021; Accepted 19 July 2021
Available online 22 July 2021
0026-265X/© 2021 Elsevier B.V. All rights reserved.

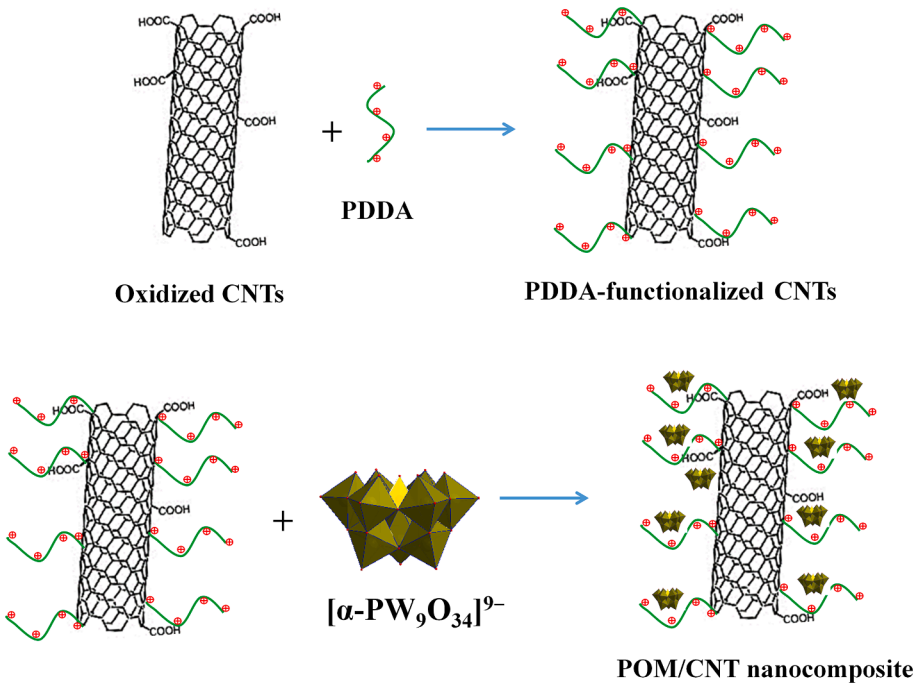

Fig. 1. The preparation route of LPOT/CNT nanocomposite.

adsorbent and selective removal of cationic pollutants compared to anionic pollutants [40,41]. Unfortunately, POMs have low surface area due to their tendency to aggregate and are difficult to use as sorbents. To solve this problem, POMs have anchored on various support such as graphene [42,43], carbon nanotubes (CNTs) [43], magnetic nanoparticles [44,45], *etc*.

In a previous work [37], $[SiW_{11}O_{39}]^{8-}$ immobilized on the surface of GO sheets and used as sorbent for the extraction of the non-steroidal anti-inflammatory drugs (NSAIDs) in the water samples. Lacunary Keggin anions are defect derivatives of saturated ones, including one or more vacant sites such as mono-lacunary, di or tri-lacunary derivatives. It is well known that lacunary derivatives are more reactive than the original Keggin anion due to the presence of multiple labile terminal oxo ligands. Meanwhile, electrostatic interaction between the positively charged substrates and these oxo-anion ligands make these reactive species more stable. Therefore, by increasing the negative charge on the lacunary derivatives from mono $[SiW_{11}O_{39}]^{8-}$ to the tri-lacunary $[PW_9O_{34}]^{9-}$, the electrostatic interactions become stronger [46].

CNTs are a kind of good sorbent that due to their unique physical and chemical properties have been widely used in sample preparation. The dispersion of POMs on the CNTs can increase the adsorption ability of POMs and the development of multi-functional material. In this work, through an efficient and facile way, the LPOT of $\{\alpha\text{-}PW_9O_{34}\}^{9-}$ was anchored on the surface of CNTs (LPOT/CNT) via positively charged poly(diallyldimethylammonium chloride) (PDDA) as the linker between CNTs and LPOTs. To the best of our knowledge, the use of LPOT/CNT nanocomposite as a sorbent has not been reported. The resulting nanocomposite (LPOT/CNT) was applied as sorbent for the D-μSPE of five commonly used OPPs in Iran (*i.e.* fenthion, diazinon, fenitrothion, profenofos, and phosalone) from fruit juice and real water samples before the gas chromatography-flame ionization detector (GC-FID).

2. Experimental

2.1. Chemicals and materials

All reagent chemicals and OPPs such as fenthion, diazinon, fenitrothion, profenofos, and phosalone, were obtained from Merck. The MWCNTs (length range 5–15 μm, outer diameter 10–20 nm) were purchase from Shenzhen Nanotech Port Co.

The stock solution of OPPs was prepared at the concentration of 100 mg L^{-1} in methanol and stored at 4 °C in the dark. The working solutions for the optimization and validation experiments were obtained daily from the stock solution by dilution with distilled water. Apple and peach juices were purchased from the market and filtered through a filter (0.45 μm). The real water samples (wastewater and river water samples) were obtained from Sabzevar, Iran, and ultimately stored at 4 °C and dark place.

2.2. Instrumentation

The chromatographic analyses were done using a GC system (Shimadzu-17A, Tokyo, Japan) equipped with a CBP-5 capillary column (25 m × 0.25 mm, 0.25 μm film thickness) and FID. The injector temperature and detector were set at 300 °C. The oven temperature programming was operated at 100 °C, held for 3 min, ramped to 280 °C at 10 °C min^{-1}, and held for 12 min. Nitrogen (99.999%) was used as a carrier gas at a 1 mL min^{-1} flow rate. Field-emission scanning electronic microscopy (FESEM) images were recorded on a MIRA3 TESCAN electron microscope. The infrared spectra were recorded with a Fourier transform spectrophotometer (Thermo Nicolet/AVATAR 370) in the range of 4000–400 cm^{-1}.

2.3. Synthesis of $Na_9[\alpha\text{-}PW_9O_{34}]\cdot 7H_2O$

The $Na_9[\alpha\text{-}PW_9O_{34}]$ was synthesized and characterized according to the procedure reported in the literature [40]. The experiment for the preparation of $Na_9[\alpha\text{-}PW_9O_{34}]$ is as follows: first sodium tungstate dihydrate (120 g, 0.36 mol) was dissolved in 150 mL of deionized water under vigorous stirring. Subsequently, 4 mL of phosphoric acid (85%) was added to the solution and stirred. In the next step, 22.5 mL of glacial acetic acid was added dropwise and stirred again for 1 h. Finally, the white precipitate was filtrated and dried by suction filtration on a medium frit.

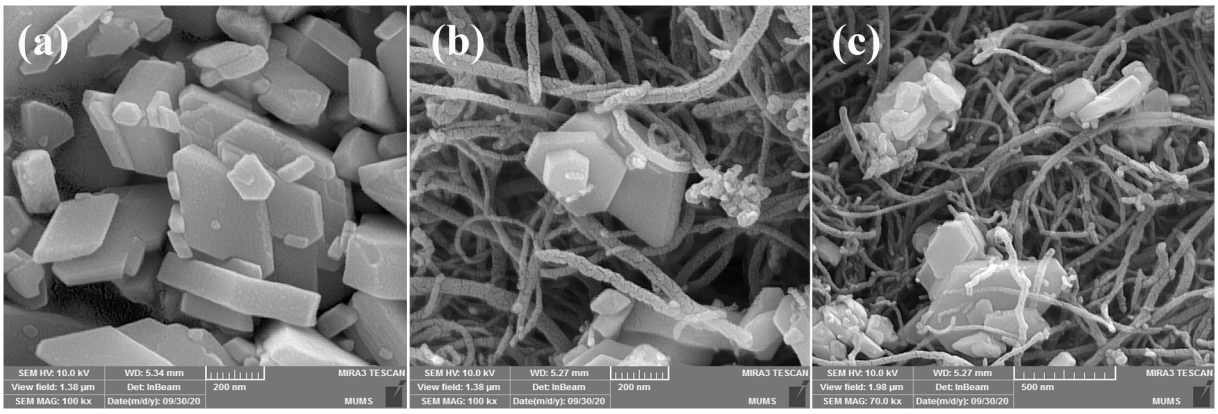

Fig. 2. FESEM images of (a) $[\alpha\text{-}PW_9O_{34}]^{9-}$ particles and (b and c) LPOT/CNT nanocomposite.

2.4. Preparation of LPOT/CNT nanocomposite

First, 1 g of pristine CNT was added to 50 mL of concentrated nitric acid (60%) and dispersed sonically. Then, the mixture was refluxed for 24 h. The oxidized CNTs were filtrated off and washed with distilled water until the pH was neutral. The resulting material dried in a vacuum at 70 °C for 12 h. For the preparation of PDDA coated CNTs, the first 50 mg of oxidized CNTs were placed in distilled water (50 mL) and sonicated for 10 min. After that, 2 mL of PDDA (20% wt% in water) was added under sonication for 90 min. Then, the obtained PDDA-wrapped CNTs were centrifuged and washed several times with deionized water. Negatively charged LPOTs can be combined with PDDA-wrapped CNTs *via* electrostatic interactions. Finally, the LPOT/CNT nanocomposite was synthesis as follows: 100 mg of PDDA-wrapped CNTs were dispersed in the 50 mL of deionized water. Then 10 mg of $[\alpha\text{-}PW_9O_{34}]^{9-}$ was added to the mixture and sonicated for 2 h. The resulting LPOT/CNT nanocomposite was filtrated off, washed with deionized water. And was dried overnight at 60 °C. The preparation procedure of the LPOT/CNT nanocomposite is illustrated in Fig. 1.

2.5. Extraction procedure

First, 15 mg of the LPOT/CNT nanocomposite was dispersed in the 20 mL of the sample solution that was spiked at 200 ng mL^{-1} of OPPs and sonicated for 2 min. After centrifugation for 5 min at 4000 rpm, desorption of extracted analytes was done by 250 µL of dichloromethane under sonication for 1.5 min. Again the mixture was centrifuged and 2 µL of supernatant was injected into the GC for the analysis.

3. Results and discussion

3.1. Characterization

To ensure proper formation of the $[\alpha\text{-}PW_9O_{34}]^{9-}$ as a *tri*-lacunary Keggin-type POMs, energy-dispersive X-ray spectroscopy (EDS), FT-IR spectroscopy, and field-emission scanning electron microscopy (FESEM) were used.

As can be seen from the FT-IR spectrum of $[\alpha\text{-}PW_9O_{34}]^{9-}$ (Fig. S1), a peak appears at 1057 cm^{-1} corresponding to the P–O_a bond (O_a = internal oxygen's). Three bonds at 749, 883, and 935 cm^{-1} are ascribed to stretching vibrations of (W–O_c), (W–O_b), and (W = O_t), respectively (O_c, bridging oxygen atoms within the edge-sharing octahedral: O_b, bridging oxygen; and O_t, terminal oxygen).

Before functionalization with PDDA, CNTs were negatively charged *via* an acid treatment procedure. Then, CNTs were functionalized with PDDA, forming positively charged PDDA-CNTs. As a consequence, the driving force for the attachment of $[\alpha\text{-}PW_9O_{34}]^{9-}$ is the electrostatic attraction between oppositely charged species (LPOT and PDDA-CNT). The FESEM image of $[\alpha\text{-}PW_9O_{34}]^{9-}$ shows that the LPOTs tend to aggregate together (Fig. 2a). The FESEM image of LPOT/CNT nanocomposite (Fig. 2b, c) indicated that the particles of $[\alpha\text{-}PW_9O_{34}]^{9-}$ are dispersed uniformly on the surface of PDDA-CNT.

The elemental composition of the LPOT/CNT nanocomposite was also investigated by using EDS and FESEM characterizations. The results of EDX analysis also confirmed the existence of tungsten and phosphorus in addition to carbon in the CNTs, indicating nonotungstophosphate polyanion was successfully grafted on the PDDA-CNTs (Fig. S2).

.

3.2. Optimization of the extraction procedure

To obtain the optimal extraction efficiency, the most important parameters that affect the efficiency of extraction such as sorbent amount, desorption conditions (i.e. desorption solvent, desorption solvent volume, and desorption time), and extraction time were investigated and optimized. All the experiments were performed in triplicate at ambient temperature and the means of the results were used for optimization. In this section, the optimized parameters for LPOT/CNT nanocomposite as sorbent are discussed.

In the D-µSPE procedure, the appropriate adsorbent amount is beneficial to allow adequate contact and transfer of the target compounds to the adsorbents. To evaluate the amount of adsorbent, different amounts of adsorbent from 5 to 20 mg were examined (Fig. S3). As the results show, the extraction efficiency increases from 5 to 15 mg, and then the extraction efficiency remains constant. These results show that with increasing the amount of LPOT/CNT nanocomposite sorbent, the contact surfaces between the sorbent and analytes increase and therefore increases the adsorption and extraction when the amount of sorbent varied from 5 to 15 mg. So, 15 mg of LPOT/CNT nanocomposite was selected for further experiments.

One of the important effective parameters in increasing the extraction efficiency is the elution conditions (i.e. desorption solvent, desorption solvent volume, and desorption time). The desorption solvent must have such sufficient strength that all the extracted analytes are eluted from the sorbent. So, it is necessary to take knowledge of the property of extraction solvent and find the most suitable one to obtain higher yields of tested analytes. Several desorption solvents such as acetonitrile, dichloromethane, ethanol, and methanol were studied. As you can see in Fig. S4, the highest desorption efficiency is shown by dichloromethane. Therefore, dichloromethane was selected as the desorption solvent.

Different volumes of dichloromethane from 100 to 500 µL were evaluated for the desorption of the analytes under sonication. Ideally, the volume of the desorption solvent should be as low as possible while being able to desorb the analytes repeatedly and quantitatively. When the volume of the desorption solvent increases from 100 to 250 µL, the

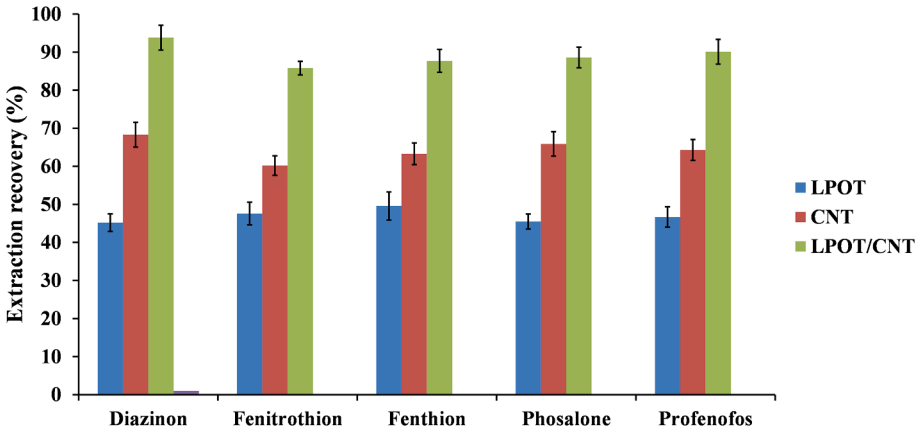

Fig. 3. Comparison of the extraction performance of CNTs (optimized extraction conditions: sample volume, 20 mL; sorbent amount, 30 mg; desorption solvent, toluene; volume desorption solvent, 500 μL; desorption time, 2 min; and extraction time, 5 min), LPOT (optimized extraction conditions: sample volume, 20 mL; sorbent amount, 50 mg; desorption solvent, dichloromethane; volume desorption solvent, 350 μL; desorption time, 3 min; and extraction time, 3 min), and LPOT/CNT (optimized extraction conditions: sample volume, 20 mL; sorbent amount, 20 mg; desorption solvent, dichloromethane; volume desorption solvent, 250 μL; desorption time, 1.5 min; and extraction time, 2 min) sorbents.

Table 1
Analytical figures of merit of the DSPE-GC-FID method using LPOT/CNT nanocomposite as a sorbent.

Analyte	Linear range (ng mL^{-1})	LOD (ng mL^{-1})	Correlation coefficient (r)	ER (%)	Repeatability (RSD%, $n = 5$)			Batch- to- batch reproducibility RSD% (n = 3)
					0.05 (ng mL^{-1})	5 (ng mL^{-1})	100 (ng mL^{-1})	
Diazinon	0.02–200	0.007	0.9945	93.8	4.2	3.7	3.3	4.5
Fenitrothion	0.05–200	0.02	0.9975	85.8	4.5	4.1	3.8	3.8
Fenthion	0.05–200	0.02	0.9939	87.7	4.7	4.3	4.0	5.0
Phosalone	0.05–200	0.02	0.9956	88.6	4.1	3.6	3.4	4.3
Profenofos	0.03–200	0.01	0.9957	90.1	4.7	4.3	4.1	4.5

amount of extraction efficiency increases, and then the extraction efficiency decreases. The 250 μL of dichloromethane was selected for further experiments.

The effect of desorption time was investigated by subjecting the analytes-enriched sorbent to sonication times ranging between 0.5 and 3 min. The extraction efficiency of OPPs reached a maximum after 1.5 min of sonication (Fig. S5). Thereafter, the extraction efficiency remained constant. Following this observation, a sonication period of 1.5 min was provided for the desorption of OPPs from LPOT/CNT nanocomposite for analysis.

The extraction time refers to the duration in which LPOT/CNT nanocomposite was in active contact with the analytes, under sonication. As shown in Fig. S6, the extraction of OPPs is most effective with 2 min of sonication. With periods longer than 2 min, the extraction efficiency of the analytes was not changed significantly. Therefore, 2 min of sonication was selected as the most favorable extraction time.

3.3. The performance of LPOT/CNT nanocomposite

To study the extraction efficiency, the performance of the CNTs,

Table 2
Determination of OPPs in real samples.

Sample	Analyte	Mean (ng mL^{-1})	Spiked amount (ng mL^{-1})					
			0.05		5		100	
			Relative recovery (%)[a]	RSD (%)	Relative recovery (%)[a]	RSD (%)	Relative recovery (%)[a]	RSD (%)
Wastewater	Diazinon	ND	97.7	5.1	98.1	4.7	98.5	4.5
	Fenitrothion	ND	97.5	5.6	98.0	5.1	98.5	4.7
	Fenthion	ND	96.7	5.3	97.9	5.0	98.3	4.6
	Phosalone	ND	97.3	5.9	98.5	5.4	98.7	5.0
	Profenofos	ND	96.9	5.4	97.4	5.1	98.0	4.9
River water	Diazinon	0.3	98.8	5.0	99.1	4.7	99.3	4.3
	Fenitrothion	ND	98.3	4.9	98.9	4.5	99.1	4.2
	Fenthion	ND	98.1	4.6	98.7	4.3	99.0	4.2
	Phosalone	ND	97.9	4.5	98.6	4.3	98.7	4.0
	Profenofos	ND	98.6	4.1	99.3	3.9	99.6	3.9
Apple juice	Diazinon	ND	95.9	5.5	96.3	5.2	97.0	4.9
	Fenitrothion	ND	96.6	5.1	97.2	4.8	97.5	4.6
	Fenthion	ND	96.5	4.7	97.3	4.3	97.6	4.0
	Phosalone	ND	95.7	4.9	96.1	4.4	96.5	4.2
	Profenofos	ND	94.2	5.0	95.9	4.7	96.3	4.3
Peach juice	Diazinon	ND	95.3	4.9	96.1	4.5	96.6	4.3
	Fenitrothion	ND	96.3	5.0	97.1	4.7	97.3	4.3
	Fenthion	ND	94.7	4.6	96.3	4.3	96.5	4.2
	Phosalone	ND	95.7	4.7	96.6	4.5	96.9	4.4
	Profenofos	ND	94.3	5.1	95.2	4.8	95.5	4.6

Table 3
Comparison of the current D-μSPE-GC-FID method with other similar methods for the determination of the OPPs.

Method	Sample	Analytes	LOD (ng mL^{-1})	Linear range (ng mL^{-1})	Organic solvent volume	RSD (%)	Reference
SPE-GC-FID (PEG-CNT coated stainless steel mesh)	Water and fruit juice samples	Diazinon	0.01	0.03–80	1 mL	3.8–5.5	[5]
		Fenitrothion	0.02	0.06–80			
		Fenthion	0.03	0.08–80			
		Phosalone	0.02	0.06–80			
		Profenofos	0.03	0.09–80			
SPE-HPLC-UV (SiO_2@Ph_4[26]aneN_4)	Tea drinks	Fenitrothion	0.1	5–500	2 mL	1.1–4.4	[47]
		Parathion	0.1	5–500			
		Fenthion	0.1	5–500			
		Phoxime	0.1	5–500			
SPE-GC–MS (three-dimensional graphene aerogel)	Water and fruit juice samples	Fenitrothion	6.218	50–1000 ng g^{-1}	8 mL	1.2–4.6	[48]
		Fenthion	2.092	50–1000 ng g^{-1}			
		Methidathion	5.045	50–1000 ng g^{-1}			
		Parathion-Methyl	7.816	50–1000 ng g^{-1}			
MDSPE–DLLME–GC–FID (toner powder)	Fruit juices	Diazinon	0.15	0.49–5000	1 mL	3–6	[49]
		Chlorpyrifos	0.26	0.87–5000			
D-μSPE-GC-FID (LPOT/CNT nanocomposite)	Water and fruit juice samples	Diazinon	0.007	0.02–200	250 μL	3.3–4.7	This study
		Fenitrothion	0.02	0.05–200			
		Fenthion	0.02	0.05–200			
		Phosalone	0.02	0.05–200			
		Profenofos	0.01	0.03–200			

LPOT, and LPOT/CNT sorbents for the extraction of OPPs. As you can see in Fig. 3, the highest extraction efficiency of the OPPs is obtained with LPOT/CNT nanocomposite. The higher extraction efficiency of the LPOT/CNT nanocomposite than CNT and LPOT can be due to the synergistic effect of LPOT and CNTs. The main idea of designing hybrids is to achieve the best characteristics of each component, try to reduce their disadvantages, getting synergic effects, and obtaining new materials with new properties. A barrier to the use of POMs as sorbent is their low surface area due to aggregation and therefore dispersion conditions are necessary. The well-dispersed LPOTs anchored on the CNT substrate increase the active surface area and the adsorption ability of LPOTs for the extraction of OPPs. Also, CNTs have high specific surface area and unique chemical structure that can be extracted analytes *via* π-stacking property and van der Waals interactions. LPOTs as active sites on the CNTs can be extracted the electron-rich OPPs *via* π-complexation and hydrogen bonding.

3.4. Method validation

The linearity, limits of detection (LODs), repeatability, and extraction recovery (ER%) of the D-μSPE-GC-FID method were evaluated (Table 1). The calibration plots for GC–FID analysis were studied by using different OPPs concentrations solution. The D-μSPE-GC-FID method for all the OPPs showed good linearity in the range of 0.02–200 ng mL^{-1} ($R > 0.9939$). The LODs defined as signal-to-noise of 3, ranged between 0.007 and 0.02 ng mL^{-1}. The precision of the developed method was determined by five consecutive D-μSPE-GC-FID method at three concentration levels (0.05, 5, and 100 ng mL^{-1}), and RSD% were in the range of 3.3 to 4.7%. Also, to study the reproducibility of the sorbent synthesis (LPOT/CNT nanocomposite), the sorbent in the different batches was synthesized for the D-μSPE of OPPs. The reproducibility for different batches was in the range of 3.8–5.0%. As can be seen from Table 1, the extraction recoveries (ER%) were 85.8–93.8%.

3.5. Analysis of real samples

The D-μSPE-GC-FID method was applied to real water samples (i.e. wastewater and river water samples), and fruit juices (*i.e.* apple and peach juice samples) to determine OPPs. The water samples were collected in bottles and stored at 4 °C in a dark place. The fruit juices were obtained from the market and filtrated with cellulose filter membranes of 0.45 μm. As you can see in Table 2, the diazinon was found in the river water sample with a concentration of 0.3 ng mL^{-1}. To investigate the matrix effect of the various samples, relative recoveries were studied at three concentration levels (0.05, 5, and 100 ng mL^{-1}). The relative recoveries of the OPPs ranged from 94.2 to 99.6% and RSDs from 3.9 to 5.9%. Therefore, it can be concluded based on the obtained results the D-μSPE-GC-FID method is an effective method for the extraction and determination of the OPPs in real samples.

The performance of the D-μSPE-GC-FID method for the extraction of OPPs was evaluated by comparing with the obtained results from SPE-GC-FID (PEG-CNT coated stainless steel mesh) [5], SPE-HPLC-UV (SiO_2@Ph_4[26]aneN_4) [47], SPE-GC–MS (three-dimensional graphene aerogel) [48], and MDSPE–DLLME–GC–FID (toner powder) [49] as summarized in Table 3. As can be seen from Table 3, the proposed method has lower LODs than those of most reported methods. It can be seen that there is no significant difference in precision obtained by the methods. Also, the D-μSPE-GC-FID method is shown a wide linear range. In addition, solvent consumption for desorption of the analytes is drastically reduced compared to other reported methods, which can be a highlight point of the proposed method. Consequently, it can be concluded that the D-μSPE-GC-FID method is suitable for the determination of OPPs in water and fruit juice samples.

4. Conclusion

In this work, the D-μSPE-GC-FID method was developed base on an LPOT/CNT nanocomposite as sorbent for the extraction and determination of OPPs in fruit juice and water samples. The results exhibited a wide linear range, good precision and recovery, and low LODs. The synthesized LPOT/CNT nanocomposite showed a higher extraction performance than CNTs and LPOT for the extraction of OPPs, due to the synergistic effect of CNTs and LPOTs in the nanocomposite. This study provides a novel strategy to effectively fabricate advanced nanocomposite composed of CNTs and LPOT that can be used as an effective sorbent for extraction of various analytes.

CRediT authorship contribution statement

Mahmood Akbari: Methodology, Investigation, Validation, Writing - original draft. **Masoud Mirzaei:** Supervision, Project administration, Writing - review & editing. **Amirhassan Amiri:** Supervision, Project administration, Writing - review & editing.

Declaration of Competing Interest

The authors declare that they have no known competing financial interests or personal relationships that could have appeared to influence the work reported in this paper.

Acknowledgments

The authors appreciate the support of the Ferdowsi University of Mashhad (No. 3/50674), Zeolite and Porous Materials Committee of Iranian Chemical Society, the Iran National Science Foundation (INSF), Iran Science Elites Federation (ISEF), and the Cambridge Crystallographic Data Centre (CCDC) for access to the Cambridge Structural Database.

Appendix A. Supplementary data

Supplementary data to this article can be found online at https://doi.org/10.1016/j.microc.2021.106665.

References

[1] Q. Li, Organophosphorus pesticides markedly inhibit the activities of natural killer, cytotoxic T lymphocyte and lymphokine-activated killer: a proposed inhibiting mechanism via granzyme inhibition, Toxicology 172 (2002) 181–190, https://doi.org/10.1016/S0300-483X(02)00004-5.

[2] A. Amiri, Solid-phase microextraction-based sol–gel technique, TrAC Trend Anal. Chem. 75 (2016) 57–74, https://doi.org/10.1016/j.trac.2015.10.003.

[3] A. Amiri, M. Baghayeri, F. Karimabadi, F. Ghaemi, B. Maleki, Graphene oxide/polydimethylsiloxane-coated stainless steel mesh for use in solid-phase extraction cartridges and extraction of polycyclic aromatic hydrocarbons, Microchim. Acta 187 (2020) 213, https://doi.org/10.1007/s00604-020-4193-z.

[4] M. Nasiri, H. Ahmadzadeh, A. Amiri, Sample preparation and extraction methods for pesticides in aquatic environments: a review, TrAC Trend Anal. Chem. 123 (2020) 115772, https://doi.org/10.1016/j.trac.2019.115772.

[5] A. Amiri, M. Baghayeri, N. Vahdati-Nasab, Effective extraction of organophosphorus pesticides using sol–gel based coated stainless steel mesh as novel solid-phase extraction sorbent, J. Chromatogr. A 1620 (2020) 461020, https://doi.org/10.1016/j.chroma.2020.461020.

[6] F.d.M. Rodrigues, P.R.R. Mesquita, L.S. de Oliveira, F.S. de Oliveira, A. Menezes Filho, P.A. de P. Pereira, J.B. de Andrade, Development of a headspace solid-phase microextraction/gas chromatography–mass spectrometry method for determination of organophosphorus pesticide residues in cow milk, Microchem. J. 98 (1) (2011) 56–61, https://doi.org/10.1016/j.microc.2010.11.002.

[7] X.-P. Lin, X.-Q. Wang, J. Wang, Y.-W. Yuan, S.-S. Di, Z.-W. Wang, H. Xu, H.-Y. Zhao, C.-S. Zhao, W. Ding, P.-P. Qi, Magnetic covalent organic framework as a solid-phase extraction absorbent for sensitive determination of trace organophosphorus pesticides in fatty milk, J. Chromatogr. A 1627 (2020) 461387, https://doi.org/10.1016/j.chroma.2020.461387.

[8] L. Du, X. Wang, T. Liu, J. Li, J. Wang, M. Gao, H. Wang, Magnetic solid-phase extraction of organophosphorus pesticides from fruit juices using NiFe2O4@polydopamine@Mg/Al-layered double hydroxides nanocomposites as an adsorbent, Microchem. J. 150 (2019) 104128, https://doi.org/10.1016/j.microc.2019.104128.

[9] M.A. Farajzadeh, A. Asghari, B. Feriduni, An efficient, rapid and microwave-accelerated dispersive liquid–liquid microextraction method for extraction and pre-concentration of some organophosphorus pesticide residues from aqueous samples, J. Food Compos. Anal. 48 (2016) 73–80, https://doi.org/10.1016/j.jfca.2016.02.007.

[10] X. Mao, Y. Wan, Z. Li, L. Chen, H. Lew, H. Yang, Analysis of organophosphorus and pyrethroid pesticides in organic and conventional vegetables using QuEChERS combined with dispersive liquid-liquid microextraction based on the solidification of floating organic droplet, Food Chem. 309 (2020) 125755, https://doi.org/10.1016/j.foodchem.2019.125755.

[11] M.Á. González-Curbelo, J. Hernández-Borges, T.M. Borges-Miquel, M.Á. Rodríguez-Delgado, Determination of organophosphorus pesticides and metabolites in cereal-based baby foods and wheat flour by means of ultrasound-assisted extraction and hollow-fiber liquid-phase microextraction prior to gas chromatography with nitrogen phosphorus detection, J. Chromatogr. A 1313 (2013) 166–174, https://doi.org/10.1016/j.chroma.2013.05.081.

[12] S. Zhao, Y. Chen, Y.-F. Song, Tri-lacunary polyoxometalates of Na8H[PW9O34] as heterogeneous Lewis base catalysts for Knoevenagel condensation, cyanosilylation and the synthesis of benzoxazole derivatives, Appl. Catal. A Gen. 475 (2014) 140–146, https://doi.org/10.1016/j.apcata.2014.01.017.

[13] T. Khezeli, A. Daneshfar, Development of dispersive micro-solid phase extraction based on micro and nano sorbents, TrAC Trend Anal. Chem. 89 (2017) 99–118, https://doi.org/10.1016/j.trac.2017.01.004.

[14] M. Ghorbani, M. Aghamohammadhassan, H. Ghorbani, A. Zabihi, Trends in sorbent development for dispersive micro-solid phase extraction, Microchem. J. 158 (2020) 105250, https://doi.org/10.1016/j.microc.2020.105250.

[15] A. Amiri, R. Tayebee, A. Abdar, F. Narenji Sani, Synthesis of a zinc-based metal-organic framework with histamine as an organic linker for the dispersive solid-phase extraction of organophosphorus pesticides in water and fruit juice samples, J. Chromatogr. A 1597 (2019) 39–45, https://doi.org/10.1016/j.chroma.2019.03.039.

[16] M. Shakourian, Y. Yamini, M. Safari, Facile magnetization of metal–organic framework TMU-6 for magnetic solid-phase extraction of organophosphorus pesticides in water and rice samples, Talanta 218 (2020) 121139, https://doi.org/10.1016/j.talanta.2020.121139.

[17] A. Targhoo, A. Amiri, M. Baghayeri, Magnetic nanoparticles coated with poly(p-phenylenediamine-co-thiophene) as a sorbent for preconcentration of organophosphorus pesticides, Microchim. Acta 185 (2017) 15, https://doi.org/10.1007/s00604-017-2560-1.

[18] R. Alizadeh, B. mashalavi, A. Yeganeh Faal, S. Seidi, Seidi Development of ultrasound assisted dispersive micro solid phase extraction based on CuO nanoplate-polyaniline composite as a new sorbent for insecticides analysis in wheat samples, Microchem. J. 168 (2021) 106422, https://doi.org/10.1016/j.microc.2021.106422.

[19] P.G. Arias, H. Martínez-Pérez-Cejuela, A. Combès, V. Pichon, E. Pereira, J. M. Herrero-Martínez, M. Bravo, Selective solid-phase extraction of organophosphorus pesticides and their oxon-derivatives from water samples using molecularly imprinted polymer followed by high-performance liquid chromatography with UV detection, J. Chromatogr. A 1626 (2020) 461346, https://doi.org/10.1016/j.chroma.2020.461346.

[20] M. Asensio-Ramos, G. D'Orazio, J. Hernandez-Borges, A. Rocco, S. Fanali, Multi-walled carbon nanotubes–dispersive solid-phase extraction combined with nano-liquid chromatography for the analysis of pesticides in water samples, Anal. Bioanal. Chem. 400 (4) (2011) 1113–1123, https://doi.org/10.1007/s00216-011-4885-7.

[21] J.-W. Zhao, Y.-Z. Li, L.-J. Chen, G.-Y. Yang, Research progress on polyoxometalate-based transition-metal-rare-earth heterometallic derived materials: Synthetic strategies, structural overview and functional applications, Chem. Commun. 52 (24) (2016) 4418–4445, https://doi.org/10.1039/C5CC10447E.

[22] M. Han, Y. Niu, R. Wan, Q. Xu, J. Lu, P. Ma, C. Zhang, J. Niu, J. Wang, A Crown-Shaped Ru-Substituted Arsenotungstate for Selective Oxidation of Sulfides with Hydrogen Peroxide, Chem. Eur. J. 24 (43) (2018) 11059–11066, https://doi.org/10.1002/chem.v24.4310.1002/chem.201800748.

[23] L.i. Chen, W.-L. Chen, X.-L. Wang, Y.-G. Li, Z.-M. Su, E.-B. Wang, Polyoxometalates in dye-sensitized solar cells, Chem. Soc. Rev. 48 (1) (2019) 260–284, https://doi.org/10.1039/C8CS00559A.

[24] Z. Li, L.-D. Lin, H. Yu, X.-X. Li, S.-T. Zheng, All-inorganic ionic porous material based on giant spherical polyoxometalates containing core-shell K6@K36-water cage, Angew. Chem. Int. Ed. 57 (48) (2018) 15777–15781, https://doi.org/10.1002/anie.201810074.

[25] D.-L. Long, R. Tsunashima, L. Cronin, Polyoxometalates: building blocks for functional nanoscale systems, Angew. Chem. Int. Ed. 49 (10) (2010) 1736–1758, https://doi.org/10.1002/anie.v49:1010.1002/anie.200902483.

[26] S. Taleghani, M. Mirzaei, H. Eshtiagh-Hosseini, A. Frontera, Tuning the topology of hybrid inorganic–organic materials based on the study of flexible ligands and negative charge of polyoxometalates: a crystal engineering perspective, Coord. Chem. Rev. 309 (2016) 84–106, https://doi.org/10.1016/j.ccr.2015.10.004.

[27] M. Arefian, M. Mirzaei, H. Eshtiagh-Hosseini, A. Frontera, A survey of the different roles of polyoxometalates in their interaction with amino acids, peptides and proteins, Dalton Trans. 46 (21) (2017) 6812–6829, https://doi.org/10.1039/C7DT00894E.

[28] Z. Khoshkhan, M. Mirzaei, H. Eshtiagh-Hosseini, M. Izadyar, J.T. Mague, M. Korabik, Two polyoxometalate-based hybrids constructed from trinuclear lanthanoid clusters with single-molecule magnet behavior, Polyhedron 194 (2021) 114903, https://doi.org/10.1016/j.poly.2020.114903.

[29] M. Mirzaei, H. Eshtiagh-Hosseini, M. Alipour, A. Frontera, Recent developments in the crystal engineering of diverse coordination modes (0–12) for Keggin-type polyoxometalates in hybrid inorganic–organic architectures, Coord. Chem. Rev. 275 (2014) 1–18, https://doi.org/10.1016/j.ccr.2014.03.012.

[30] Z. Li, X.-X. Li, T. Yang, Z.-W. Cai, S.-T. Zheng, Four-Shell Polyoxometalates Featuring High-Nuclearity Ln26Clusters: Structural Transformations of Nanoclusters into Frameworks Triggered by Transition-Metal Ions, Angew. Chem. Int. Ed. 56 (10) (2017) 2664–2669, https://doi.org/10.1002/anie.201612046.

[31] X. Chen, Y.e. Zhou, V.A.L. Roy, S.-T. Han, Evolutionary Metal Oxide Clusters for Novel Applications: Toward High-Density Data Storage in Nonvolatile Memories, Adv. Mater. 30 (3) (2018) 1703950, https://doi.org/10.1002/adma.v30.310.1002/adma.201703950.

[32] L. Cronin, A. Müller, From serendipity to design of polyoxometalates at the nanoscale, aesthetic beauty and applications, Chem. Soc. Rev. 41 (2012) 7333–7334, https://doi.org/10.1039/c2cs90087d.

[33] Y.-N. Gu, Y.i. Chen, Y.-L. Wu, S.-T. Zheng, X.-X. Li, A Series of Banana-Shaped 3d–4f Heterometallic Cluster Substituted Polyoxometalates: Syntheses, Crystal Structures, and Magnetic Properties, Inorg. Chem. 57 (5) (2018) 2472–2479, https://doi.org/10.1021/acs.inorgchem.7b02728.

[34] X.-X. Li, W.-H. Fang, J.-W. Zhao, G.-Y. Yang, The first 3-connected SrSi2-type 3D chiral framework constructed from Ni6PW9 building units, Chem. Eur. J. 21 (6) (2015) 2315–2318, https://doi.org/10.1002/chem.201405290.

[35] N.C. Coronel, M.J. da Silva, Lacunar Keggin Heteropolyacid Salts: Soluble, Solid and Solid-Supported Catalysts, J. Clust. Sci. 29 (2) (2018) 195–205, https://doi.org/10.1007/s10876-018-1343-0.
[36] M. Ammam, Polyoxometalates: Formation, structures, principal properties, main deposition methods and application in sensing, J. Mater. Chem. A 1 (2013) 6291–6312, https://doi.org/10.1039/c3ta01663c.
[37] A. Amiri, M. Mirzaei, S. Derakhshanrad, A nanohybrid composed of polyoxotungstate and graphene oxide for dispersive micro solid-phase extraction of non-steroidal anti-inflammatory drugs prior to their quantitation by HPLC, Microchim. Acta 186 (2019) 534, https://doi.org/10.1007/s00604-019-3694-0.
[38] D.-L. Long, E. Burkholder, L. Cronin, Polyoxometalate clusters, nanostructures and materials: From self assembly to designer materials and devices, Chem. Soc. Rev. 36 (1) (2007) 105–121, https://doi.org/10.1039/B502666K.
[39] M. Arab Fashapoyeh, M. Mirzaei, H. Eshtiagh-Hosseini, A. Rajagopal, M. Lechner, R. Liu, C. Streb, Photochemical and electrochemical hydrogen evolution reactivity of lanthanide-functionalized polyoxotungstates, Chem. Commun. 54 (74) (2018) 10427–10430, https://doi.org/10.1039/C8CC06334F.
[40] F.-Y. Yi, W. Zhu, S. Dang, J.-P. Li, D. Wu, Y.-H. Li, Z.-M. Sun, Polyoxometalates-based heterometallic organic-inorganic hybrid materials for rapid adsorption and selective separation of methylene blue from aqueous solutions, Chem. Commun. 51 (16) (2015) 3336–3339, https://doi.org/10.1039/C4CC09569C.
[41] S. Derakhshanrad, M. Mirzaei, C. Streb, A. Amiri, C. Ritchie, Polyoxometalate-Based Frameworks as Adsorbents for Drug of Abuse Extraction from Hair Samples, Inorg. Chem. 60 (3) (2021) 1472–1479, https://doi.org/10.1021/acs.inorgchem.0c0276910.1021/acs.inorgchem.0c02769.s001.
[42] K. Kume, N. Kawasaki, H. Wang, T. Yamada, H. Yoshikawa, K. Awaga, Enhanced capacitor effects in polyoxometalate/graphene nanohybrid materials: a synergetic approach to high performance energy storage, J. Mater. Chem. A 2 (11) (2014) 3801–3807, https://doi.org/10.1039/C3TA14569G.
[43] Y. Ji, L. Huang, J. Hu, C. Streb, Y.-F. Song, Polyoxometalate-functionalized nanocarbon materials for energy conversion, energy storage and sensor systems, Energy Environ. Sci. 8 (3) (2015) 776–789, https://doi.org/10.1039/C4EE03749A.
[44] A. Amiri, F.M. Zonoz, A. Targhoo, H.R. Saadati-Moshtaghin, Enrichment of phenolic compounds from water samples by using magnetic Fe_3O_4 nanoparticles coated with a Keggin type heteropoly acid of type $H_6[BFe(_{OH2})W_{11}O_{39}]$ as a sorbent, Microchim. Acta 184 (4) (2017) 1093–1101, https://doi.org/10.1007/s00604-017-2103-9.
[45] A. Misra, C. Zambrzycki, G. Kloker, A. Kotyrba, M.H. Anjass, I. Franco Castillo, S. G. Mitchell, R. Güttel, C. Streb, Water Purification and Microplastics Removal Using Magnetic Polyoxometalate-Supported Ionic Liquid Phases (magPOM-SILPs), Angew. Chem. Int. Ed. 59 (4) (2020) 1601–1605, https://doi.org/10.1002/anie.v59.410.1002/anie.201912111.
[46] M. Samaniyan, M. Mirzaei, R. Khajavian, H. Eshtiagh-Hosseini, C. Streb, Heterogeneous Catalysis by Polyoxometalates in Metal-Organic Frameworks, ACS Catal. 9 (11) (2019) 10174–10191, https://doi.org/10.1021/acscatal.9b03439.
[47] L.i. Gao, L. Liu, Y. Sun, W. Zhao, L. He, Fabrication of a novel azamacrocycle-based adsorbent for solid-phase extraction of organophosphorus pesticides in tea drinks, Microchem. J. 153 (2020) 104364, https://doi.org/10.1016/j.microc.2019.104364.
[48] F. Huo, H. Tang, X. Wu, D. Chen, T. Zhao, P. Liu, L. Li, Utilizing a novel sorbent in the solid phase extraction for simultaneous determination of 15 pesticide residues in green tea by GC/MS, J. Chromatogr. B 1023–1024 (2016) 44–54, https://doi.org/10.1016/j.jchromb.2016.04.053.
[49] M.A. Farajzadeh, A. Mohebbi, Development of magnetic dispersive solid phase extraction using toner powder as an efficient and economic sorbent in combination with dispersive liquid–liquid microextraction for extraction of some widely used pesticides in fruit juices, J. Chromatogr. A 1532 (2018) 10–19, https://doi.org/10.1016/j.chroma.2017.11.048.